Frequency domain interferometer simulation with higher-order spatial modes

A Freise†‡, G Heinzel§, H Lück§, R Schilling§, B Willke§ and K Danzmann§

‡ European Gravitational Observatory, Via E. Amaldi, 56021 Cascina (PI), Italy
§ Max-Planck-Institute for Gravitational Physics (Albert-Einstein-Institute) and University of Hannover, Callinstr. 38, D-30167 Hannover, Germany

Abstract. FINESSE is a software simulation allowing one to compute the optical properties of laser interferometers used by interferometric gravitational-wave detectors today. This fast and versatile tool has already proven to be useful in the design and commissioning of gravitational-wave detectors. The basic algorithm of FINESSE numerically computes the light amplitudes inside an interferometer using Hermite-Gauss modes in the frequency domain. In addition, FINESSE provides a number of commands for easily generating and plotting the most common signals including power enhancement, error and control signals, transfer functions and shot-noise-limited sensitivities.

Among the various simulation tools available to the gravitational wave community today, FINESSE provides an advanced and versatile optical simulation based on a general analysis of user-defined optical setups and is quick to install and easy to use.

† To whom correspondence should be addressed

1. Introduction

The recently built interferometric gravitational-wave detectors use a new class of laser interferometers: new topologies have been formed combining well-known interferometer types such as Michelson or Fabry-Perot interferometers. In addition, the search for gravitational waves requires optical systems with a very long baseline, a large circulating power and an extreme stability. The properties of this new class of laser interferometers have been subject to extensive research. FINESSE is an interferometer simulation that has been developed as a tool for designing and validating interferometer topologies and, especially, the necessary control configurations‡. It is currently available in the Internet [1]; the package contains the program itself, several examples and detailed documentation (a graphical user interface for FINESSE is available also [2]). FINESSE is part of a collection of simulation tools for advanced interferometry available to the gravitational wave community [3].

The main task of the program lies in the computation of the amplitudes of light fields in an user-defined optical setup. This is done by transforming the user's description of the interferometer into a set of linear equations, which is then solved numerically using a well-known algorithm for sparse matrices [4]. With the light amplitudes known at each location inside the interferometer, the 'optical problem' is completely solved. For fast simulations, FINESSE provides many features for automatically generating the most common interferometer output signals. A variety of output signals can be computed including field amplitudes, light intensity and light power, optionally demodulated by up to 5 Fourier frequencies. In fact, almost every parameter of the interferometer description can be tuned during the simulation. FINESSE automatically calls Gnuplot (a free graphics software [5]) to create 2D or 3D plots of the output data. An optional text output provides information about the optical setup such as mode mismatch coefficients, eigen-modes of cavities and beam sizes.

2. Mathematical description of interferometers

Various techniques for computing the properties of optical systems exist. One principal aim in developing FINESSE was to create a fast and accurate tool that is easy to use, and techniques applied here were chosen accordingly. At the same time special approximations were to be excluded to provide an easy derivation of quantitative error estimates and a tool that is as flexible and versatile as possible. All interferometric detectors today employ optical systems with similar features: a) In normal operating condition, all parameters such as mirror positions, angles and light powers should be as constant as possible (by virtue of sophisticated stabilisation systems). b) The light fields inside the interferometer can be understood as a sum of the laser input light at a fixed wavelength and different field components with small frequency offsets

‡ By *control configurations* we refer to the various possible methods for stabilising a chosen optical setup to the desired operating point, both for longitudinal and alignment degrees of freedom.

(typically 1 Hz to 100 MHz). c) The optical systems are designed such that the light beams have a small divergence angle and are always small compared to the (main) optical elements. Such systems can be well described using the frequency domain and the paraxial approximation. Both methods are well-known, provide relatively intuitive results and were thus chosen as a baseline for FINESSE. Special analysis tasks such as the lock acquisition process or non-linear couplings require a time-domain analysis. When the paraxial approximation cannot be used, more general models for beam propagation, such as FFT propagation, have to be employed. Unfortunately, these methods require more computing power than a paraxial analysis in the frequency domain.

The paraxial approach is a straightforward extension to a plane-wave analysis; for a better understanding the basic principles of FINESSE are explained in the following using plane waves only. Further on, the necessary extensions for using higher-order transversal modes are explained.

2.1. The plane-wave approximation

In the plane-wave approximation the geometric properties transverse to the optical axis are ignored; thus the analysis becomes one-dimensional. A light field at one point in space can be described as a sum of frequency components:

$$E(t) = \sum_j a_j \, \exp\left(\mathrm{i}\,\omega_j\, t\right) \tag{1}$$

with ω_j as the angular frequency of the light field and a_j as complex coefficients, holding the amplitude and phase information. A common method for analysing optical systems is to define linear coupling coefficients for the (complex) amplitudes of the electric field component of the light field locally for every optical component. For example, the coupling coefficients for a light field (plane wave) at a plane, partly reflecting surface can be given as:

$$\begin{pmatrix} \mathrm{Out1} \\ \mathrm{Out2} \end{pmatrix} = \begin{pmatrix} r & \mathrm{i}\,t \\ \mathrm{i}\,t & r \end{pmatrix} \begin{pmatrix} \mathrm{In1} \\ \mathrm{In2} \end{pmatrix}$$

with r and t as the amplitude coefficients for reflectance and transmittance of the surface, 'In' as the incoming light fields and 'Out' the outgoing light fields§. In the plane-wave mode the interferometer can be built from the following components: mirror, beam splitter, free propagation ('space') , input light ('laser'), electro-optic modulator, Faraday isolator and photo diodes. All together, the linear couplings of the optical components in a user-defined setup form a set of linear equations for the light field amplitudes. It is solved numerically by FINESSE to obtain the steady-state solution (light amplitude for every location in the optical system) from which the output signals are generated with respect to the defined detectors.

§ The phase change upon reflection can also be implemented differently; this representation was chosen for its symmetry [6].

Lengths and tunings: Interferometers often employ propagation of light fields over large distances (e.g. meters to kilometers) while at the same time the interference conditions depend on the microscopic differences between two lengths (e.g. less than a micrometer). To be able to accurately describe the system on both scales, any distance D is given by two numbers [6]: the length L, defined as the multiple of the laser wavelength λ_0 yielding the smallest difference to D, and a microscopic *tuning* ϕ defined as the remaining difference between L and D (ϕ is given in radians with 2π referring to one wavelength). In FINESSE lengths are used as a parameter of free propagation, whereas tunings are introduced as local parameters of mirrors and beam splitters.

Static response, frequency response: Any interferometer output signal can be computed as a function of a quasi-static parameter change (henceforth called *static signal*) or as a function of the Fourier frequency of a test signal (henceforth referred to as *transfer function*). Whereas the static response can be used to search for operating points with suitable control signals, the transfer functions are commonly used to compute the sensitivity of the system and the coupling of various noise sources into the gravitational wave signal. In addition, transfer functions provide the necessary data for the design of the frequency response of the control system filters.

Modulation, demodulation: Modulation of a light field (in phase, amplitude or frequency) can be implemented by adding new field components, so-called sidebands, with a frequency offset to the carrier equal to integer multiples of the modulation frequency.

The interferometer matrix has then to be solved sequentially for all existing frequency components. In general, a large number of fields with different Fourier frequencies is present on each detector. Often the detected photo current is to be demodulated by one or more frequencies and subsequently low pass filtered to generate the desired output signal. In the frequency domain the demodulation (which, in the time domain, represents a multiplication with a periodic function, here a sine wave) plus the additional low pass can be realized by a selection of the respective beat signals between the field amplitudes. For example, a signal proportional to the photo current of a detector illuminated by a field as given in Equation 1 is:

$$S_0 \; = \; |E|^2 \; = \; \sum_{i=0}^{N}\sum_{j=0}^{N} a_i a_j^* \; e^{i\,(\omega_i-\omega_j)\,t} \; =: \sum_{i=0}^{N}\sum_{j=0}^{N} A_{ij} \; e^{i\,\omega_{ij}\,t} \tag{2}$$

After a single demodulation at frequency ω_x the low frequency component of the signal can be written as:

$$S = \sum_i \sum_j \text{Re}\left\{A_{ij} \; e^{-i\,\varphi_x}\right\} \quad \text{for} \quad \{i,j \mid i,j \in \{0,\dots,N\} \; \wedge \; \omega_{ij} = \omega_x\} \tag{3}$$

with φ_x as the demodulation phase.

2.2. The paraxial approximation: Hermite-Gauss modes

The plane-wave approximation provides information about longitudinal degrees of freedom of an interferometric detector only. The alignment of the optical components, however, plays an important role for the stability and noise performance of an interferometer. Furthermore, the transverse properties of the optical components often affect the longitudinal signals also. These effects can be computed using Hermite-Gauss modes that are exact solutions of the paraxial wave equation. Depending on the amount of deviation (misalignment or mismatch), a number of higher-order modes describe a paraxial system in a good approximation. FINESSE offers two additional components in the Hermite-Gauss mode: the thin lens and the beam analyser used to plot the shape of the beam on the detector. In addition, attributes for mirrors and beam splitters can now be set, namely radius of curvature and angle of misalignment.

Tracing the beam: In the paraxial approximation the electrical field can be described as:

$$E(t, x, y, z) = \sum_j \sum_{n,m} a_{jnm}\, u_{nm}(x, y, z)\, \exp\left(\mathrm{i}\left(\omega_j\, t - k_j z\right)\right) \tag{4}$$

with $u_{nm}(x, y, z)$ describing the spatial properties of the Hermite-Gauss modes and a_{jnm} as complex amplitude factors ($k_j = \omega_j/c$). Each set of Hermite-Gauss modes u_{nm} represents a complete set uniquely described by the so-called Gaussian beam parameter $q_0 = \mathrm{i}\, z_\mathrm{R} - z_0$, with z_R being the Rayleigh range and z_0 the position of the beam waist.

In a general optical setup the shape of the beams is not known a priori but depends on the resonance condition of cavities. On the other hand, a set of base functions has to be defined before starting the calculation. The choice of possible q_0 values is critical; even for only small deviations of q_0 from the optimum beam parameter the number of higher-order transverse modes that have to be included in the simulation increases significantly. To avoid numeric errors and to optimise the simulation speed the Gaussian beam parameters should be set with great care.

A possible method for finding reasonable beam parameters for every location in the interferometer (every *node* in FINESSE) is to first set the beam parameters where they are known intuitively and then derive the remaining beam parameters from these initial ones: The user can define the beam parameters directly for a given location in the optical setup, especially for the laser outputs. In addition, FINESSE can compute the eigen-modes of (geometrically stable) cavities and sets the respective beam parameters on every node that is part of the respective cavity. A beam-tracing algorithm is used to derive and set beam parameters for the remaining nodes. *Trace* in this context means that a beam starting at a node with an already known beam parameter is propagated through the optical system and the beam parameter is transformed according to the optical elements passed using the ABCD matrix-formalism [7].

If the interferometer is confined to a plane as in FINESSE, it is convenient to use two beam parameters: q_s for the sagittal plane and q_t for the tangential plane so that

the Hermite-Gauss modes can be written as:

$$u_{nm}(x, y, z, q_0) = u_n(x, z, q_t) \, u_m(y, z, q_s) \tag{5}$$

Also geometrical attributes such as radius of curvature or misalignment angles can be given for the sagittal and tangential planes separately. This allows one to include optical elements with astigmatism in the analysis.

Coupling coefficients: During free propagation the Hermite-Gauss modes are not coupled. Coupling is introduced in general whenever the interference between two beams is to be computed. In that case one beam has to be described in the base set of Hermite-Gauss modes of the other beam. This change of base system introduces couplings between the TEM modes except for the special case of perfect *alignment* and *matching*. 'Matching' refers to the difference in the Gaussian beam parameter q_0 of the two beams. So-called coupling coefficients have to be computed for every mirror and beam splitter. A set of Hermite-Gauss modes u_{nm} characterised by the beam parameter q_0 can be expanded using a different set of Hermite-Gauss modes [8]:

$$u_{nm}(q) \exp\left(i\left(\omega t - kz\right)\right) = \sum_{n',m'} k_{nmn'm'} u_{n'm'}(q') \exp\left(i\left(\omega t - kz'\right)\right) \tag{6}$$

where $u_{n'm'}$ represents Hermite-Gauss modes with a different beam parameter q_0' in a coordinate system x', y', z' that is rotated around the y axis by the *misalignment angle* γ. The coupling coefficients are thus given by the following projection:

$$k_{nmn'm'} = \exp\left(i\, 2kz' \sin^2\left(\frac{\gamma}{2}\right)\right) \iint dx' dy' \, u_{n'm'} \exp\left(i\, kx' \sin \gamma\right) u_{nm}^* \tag{7}$$

For small misalignments ($\gamma \ll 1$) the coupling coefficients can be split into $k_{nmn'm'} \approx k_{nn'} k_{mm'}$. In [8] the above projection integral is partly solved and the coupling coefficients are given by simple sums as functions of γ and the mode mismatch parameter K, which are defined as:

$$K = \tfrac{1}{2}(K_0 + i\, K_2) \quad \text{with:}$$
$$K_0 = (z_R - z_R')/z_R', \qquad K_2 = ((z - z_0) - (z' - z_0'))/z_R' \tag{8}$$

Table 1 shows the coupling coefficients for two special cases as an example.

$k_{nn'}$	0	1	2
0	ab	0	$\frac{1}{\sqrt{2}}ab^3 K^*$
1	0	$a^3 b^3$	0
2	$\frac{-1}{\sqrt{2}}ab^3 K$	0	$a^5 b^5 - \frac{1}{2}ab^5 |K|^2$

$k_{nn'}/d$	0	1	2
0	1	$-X^*$	0
1	X	1	$-\sqrt{2}X^*$
2	0	$\sqrt{2}X$	1

Table 1. The above tables give the coupling coefficients for two special cases and mode numbers $n, n' \leq 2$: the left table refers to perfect alignment but mismatch using $a = (1 + K_0)^{1/4}$ and $b = (1 + K^*)^{-1/2}$, whereas the right table gives the coefficients for small misalignments and no mismatch with $X = -q \sin(\gamma)/w_0$ and $d = \exp(-|X|^2/2)$ (terms of order X^2 or higher have been omitted in this example).

Detectors: The Hermite-Gauss modes (as they are used here) are ortho-normal. Therefore the photo current upon detection on a single-element photo diode (for simplicity shown here for one frequency component only) is proportional to:

$$S = \sum_{n,m} a_{nm} a_{nm}^* \tag{9}$$

More interesting for the Hermite-Gauss modes are different detector types that are sensitive to the shape of the beam, such as split photo detectors. FINESSE can be used with such detectors of arbitrary design by defining the *beat coefficients*. For an arbitrary split detector the respective signal is computed as:

$$S = \sum_{n,m} \sum_{n',m'} c_{nmn'm'} a_{nm} a_{n'm'}^* \tag{10}$$

with c as the beam coefficient matrix. For example, a detector split in the x direction is usually set up to detect the difference between the two halves thus being sensitive only to the beat signals of symmetric with asymmetric modes (in the x-direction). The coefficients thus are:

$$c_{nmn'm'} = \begin{cases} 1 \text{ when } (n+1)+(n'+1) \text{ is odd and } m = m' \\ 0 \text{ otherwise} \end{cases} \tag{11}$$

The subsequent demodulation of the signal is performed exactly as in the plane-wave mode. Using split detectors the control signals for automatic alignment systems or other similar geometrical control systems can be computed.

3. Results and validation

Being a versatile simulation tool, FINESSE is based on a complex code both with respect to the programming itself and to the mathematical description of the physics. Careful testing is necessary to gain a high level of confidence with respect to the correctness of the results.

FINESSE has been subject to many implicit and explicit tests during its development and use: The plane-wave analysis with FINESSE was compared against a number of algebraic calculations of simple interferometers and cavities. Such tests should provide a good validation since the program is not tailored to any special topology or configuration. In order to test the Hermite-Gauss extensions, the simulation results had to be compared to other optical simulations: The propagation of Gaussian beam and the functioning of the beam trace algorithm could be verified using OptoCad [9]. Coupling coefficients generated by direct numerical integration were used to verify and validate the actual implementation derived from [8]. Finally, complex examples of analyses with higher-order modes were compared to the result of an FFT propagation code.

In addition, the simulated data obtained with FINESSE have been compared successfully with experimental data during the commissioning of GEO 600 [10]. On its own, such a comparison does not represent a sufficient test but confirms the dedicated tests mentioned above. The following example shows one of the first employments

of FINESSE to understand data from the Power-Recycled Michelson interferometer of GEO 600. Figure 1 shows measured and computed signals for the Power-Recycled Michelson interferometer: The Power-Recycled cavity (PRC) was locked and the Michelson interferometer (MI) was freely passing through dark fringes. Zero time indicates the center of the respective dark fringe. The left column shows three typical measured fringes; each graph shows the Michelson-interferometer error signal and the PRC visibility, respectively. It can be seen that the size of the center part of both signals strongly varies, whereas the signal shape far away from the center remains similar. The 'double dip' in the PRC visibility is due to the changing reflectance of the Michelson interferometer: It is really highly reflective only at the dark fringe so that the PRC becomes over-coupled as designed. If the Michelson interferometer is moving away from the dark fringe, its reflectance is decreased. At some point the PRC becomes impedance-matched where the visibility is minimised. By further decreasing the MI reflectance, the visibility increases; the cavity becomes under-coupled. Thus, a full fringe of the Michelson interferometer results in a double structure, as seen in Figure 1, with the minima indicating the impedance-matched states.

Simulations with FINESSE have been used to understand the signal shapes. The right column in Figure 1 shows the computed signals. The parameters of the simulations were adjusted as follows: The general input file describing the GEO 600 optical setup includes measured parameters if available and nominal parameters otherwise. To obtain a computed dark-fringe pattern similar to the observed ones, the radius of curvatures of the end mirrors (which were not known accurately) were adjusted accordingly in the simulation. The computed MI error point and the PRC visibility signals matched the measured signals with the strong center very well (top graph in Figure 1). It turned out that the form of the computed signals could be matched to the measured signals by introducing a misalignment of the end mirrors into the simulation (Figure 1 middle and bottom). Both deviations were later determined by further measurements: The radii of curvature of the end mirrors deviated from the specification as predicted by the simulation, and the varying central shape of the signal at the dark fringe was caused by an unexpected small suppression of the tilt movement of the beam splitter, which has a similar effect on the output signals as a differential tilt movement of the end mirrors.

The simulations helped to identify and characterise these defects and showed that the Michelson interferometer otherwise worked as expected. In addition, it became clear that a good and stable alignment of the interferometer mirrors is necessary for obtaining a proper error signal.

FINESSE has been widely used in several projects; however, it has been most frequently utilised during the commissioning of GEO 600. Some of these simulation results can be found in this issue [11, 12, 13, 14] and in [15].
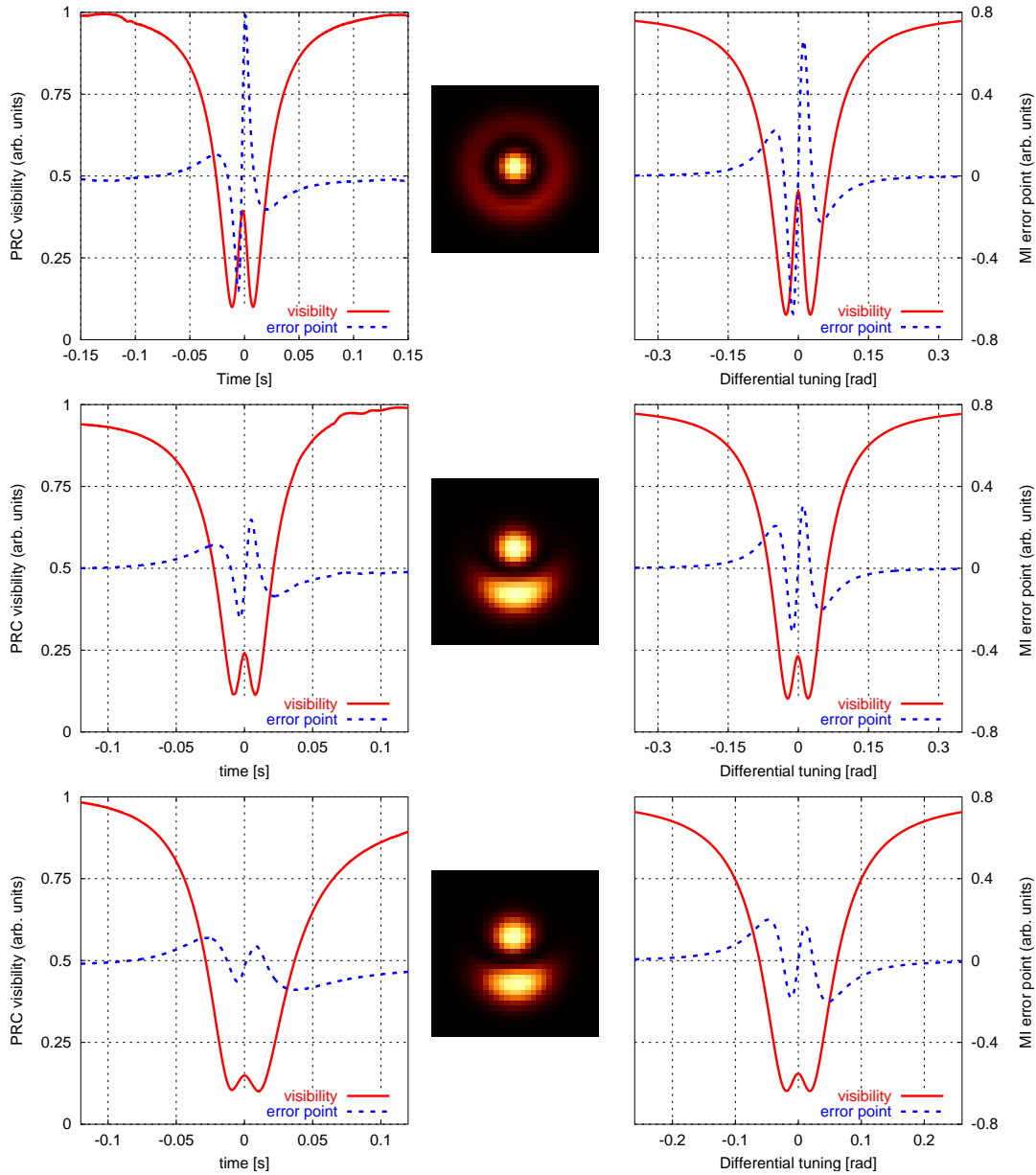
Figure 1. Measurement and simulation of Michelson-interferometer error signals: The left column shows measured signals for three typical fringes of the Michelson interferometer; each graph shows the MI error point and the PRC visibility (the fraction of the light power reflected by the cavity) while the Michelson interferometer passes through a dark fringe. The right column shows respective signals obtained by a FINESSE simulation. From top to bottom, the simulations were done for increasing misalignments of the end mirrors ($0.2\,\mu$rad, $3\,\mu$rad and $4\,\mu$rad). The center column shows the corresponding dark fringe pattern computed by the simulation.

Acknowledgments

References

[1] Freise A 1999 *Finesse* http://www.rzg.mpg.de/~ adf
[2] Harms J 2002 *Luxor* http://www.aei.mpg.de/~ jah
[3] http://www.phys.ufl.edu/LIGO/LIGO/STAIC.html
[4] Kundert K S and Sangiovanni-Vincentelli A 1988 University of California, Berkeley
[5] Williams T and Kelley C *Gnuplot* http://www.gnuplot.info
[6] Heinzel G 1999 Ph.D. Thesis, University of Hannover
[7] Siegman A E 1986 *Lasers* University Science Books, Mill Valley
[8] Bayer-Helms F 1984 *Appl. Opt.* **23** 1369–1380
[9] Schilling R 2002 *OptoCad* internal note
[10] Willke B *et al Class. Quantum Grav.* this issue
[11] Lück H *et al Class. Quantum Grav.* this issue
[12] Malec M *et al Class. Quantum Grav.* this issue
[13] Grote G *et al Class. Quantum Grav.* this issue
[14] Rakhmanov M *et al Class. Quantum Grav.* this issue
[15] Freise A 2003 Ph.D. Thesis, University of Hannover
      http://www.amps.uni-hannover.de/dissertationen/freise_diss.pdf